

BRIEF REPORT



Comparative immunologic characterization of autoimmune giant cell myocarditis with ipilimumab

Alexandre Reuben^{a,##}, Mariana Petaccia de Macedo^{b,###}, Jennifer McQuade^c, Aron Joon^d, Zhiyong Ren^{e,†}, Tiffany Calderone^b, Brandy Conner^b, Khalida Wani^b, Zachary A. Cooper^{a,f,i}, Hussein Tawbi^c, Michael T. Tetzlaff^{b,e}, Robert F. Padera^g, Jean-Bernard Durand^h, Alexander J. Lazar^{ib,b,e,*}, Jennifer A. Wargo^{a,f,*}, and Michael A. Davies^{b,c,i,*}

^aDepartment of Surgical Oncology, The University of Texas MD Anderson Cancer Center, Houston, Texas, USA; ^bTranslational Molecular Pathology, The University of Texas MD Anderson Cancer Center, Houston, Texas, USA; ^cMelanoma Medical Oncology, The University of Texas MD Anderson Cancer Center, Houston, Texas, USA; ^dBiostatistics, The University of Texas MD Anderson Cancer Center, Houston, Texas, USA; ^ePathology, The University of Texas MD Anderson Cancer Center, Houston, Texas, USA; ^fGenomic Medicine, The University of Texas MD Anderson Cancer Center, Houston, Texas, USA; ^gDepartment of Pathology, Brigham & Women's Hospital, Harvard Medical School, Boston, MA, USA; ^hCardiology, The University of Texas MD Anderson Cancer Center, Houston, Texas, USA; ⁱSystems Biology, The University of Texas MD Anderson Cancer Center, Houston, Texas, USA

ABSTRACT

Autoimmune myocarditis is a rare but often fatal toxicity of checkpoint inhibitor immunotherapy. To improve the understanding of this complication, we performed immune profiling on post-mortem tissue from a patient with metastatic melanoma who had steroid-responsive hepatitis, steroid-refractory myocarditis, and shrinking lung metastases after ipilimumab treatment. Histological analysis of heart tissue demonstrated findings consistent with giant cell myocarditis (GCM). The immune infiltrate in the heart was largely comprised of CD4+ T cells, whereas the liver had very few T cells, and CD8+ T cells were predominant in the responding lung metastases. TCR sequencing identified high T cell clonality in the lung metastases. The TCR repertoire showed low clonality in the heart and minimal overlap with the liver (1.2%), but some overlap with lung metastases (9.9%). Transcriptional profiling identified several potential mediators of increased inflammation in the heart. These findings provide new insights into the pathogenesis of autoimmune myocarditis with ipilimumab.

ARTICLE HISTORY

Received 26 June 2017
Revised 23 July 2017
Accepted 24 July 2017

KEYWORDS

Ipilimumab; Melanoma; Myocarditis

Introduction

The anti-CTLA-4 checkpoint inhibitor ipilimumab is an FDA-approved immunotherapy for patients with stage III and stage IV melanoma.¹⁻⁴ Treatment with ipilimumab is associated with the development of grade 3-4 toxicities in ~25% of patients treated with the 3 mg/kg dose approved for patients with stage IV disease, and in ~50% of patients treated with 10 mg/kg in the adjuvant setting.¹⁻⁴ The majority of these toxicities are autoimmune in nature, most commonly affecting the gastrointestinal, skin and endocrine organ systems, and usually resolve with immunosuppressants.

Autoimmune myocarditis is a rare but often fatal adverse event of ipilimumab treatment. Currently there is scarce histological, immune, or molecular information about ipilimumab-related myocarditis. Here, we report a fatal case of steroid-refractory autoimmune myocarditis in a patient with metastatic melanoma receiving ipilimumab treatment. Our report includes characterization of the inflammation and infiltration of cardiac tissue by immunohistochemistry (IHC), T cell receptor (TCR) sequencing and immune-related gene expression



profiling. Comparative analysis of other tissues from the same patient were performed, including a responding melanoma lung metastasis and tissue from the liver, which was initially inflamed but improved with steroid treatment. The results of these analyses provide new insights into the basis of ipilimumab-induced autoimmune myocarditis and suggest a potentially distinct pathogenesis from myocarditis induced by anti-PD-1.


Materials and methods

This study was approved by The University of Texas MD Anderson Cancer Center's Institutional Review Board (IRB).

Pathological review

Autopsy findings were retrieved from the clinical report performed by one of the authors (AJL). Microscopic evaluation was performed on hematoxylin and eosin (H&E) slides from The University of Texas MD Anderson Cancer Center. Clinical

CONTACT Michael A. Davies  mdavies@mdanderson.org  University of Texas MD Anderson Cancer Center, 1515 Holcombe, Unit 0430, Houston, Texas, USA 77030.

 Supplemental data for this article can be accessed on the [publisher's website](#).

[†]Now at AtlantiCare, Atlantic City, NJ, USA.

[‡]Now at MedImmune, Gaithersburg, MD, USA.

[§]Now at Department of Pathology, AC Camargo Cancer Center, São Paulo, Brazil.

^{##}These authors contributed equally.

^{*}These authors shared senior authorship.

© 2017 Taylor & Francis Group, LLC

data and selected slides were reviewed by a specialized cardiac pathologist (RFP).

Viral and fungal testing

Bacterial, mycobacterial, fungal and virus cultures were performed in MD Anderson's CLIA certified laboratory.

Immunohistochemistry studies

The immunohistochemistry reactions for CD3 (polyclonal - Dako), CD4 (4B12 - Thermo Scientific), CD8 (C8/144B - Thermo Scientific), CD20 (L-26 - Dako), CD68 (PG-M1 - Dako), CD45RO (UCHL1 - Leica) and FoxP3 (clone 206D - BioLegend) were performed on 4 μ m thick sections that were cut from Formalin Fixed Paraffin Embedded (FFPE) tissue blocks as described previously.⁵

T cell receptor sequencing

DNA was extracted from autopsy tissues from the heart, liver, and lung and the CDR3 variable region of the β chain of the T cell receptor was amplified and sequenced using ImmunoSeq (Adaptive Biotechnologies, Seattle, WA) as described previously.⁶

Gene expression profiling

Gene expression profiling was performed on RNA from the center, periphery, and whole heart, liver and lung necrotic samples using the NanoString nCounter System (NanoString technologies, Seattle, WA) using a commercial codeset (nCounter Human Immunology V2) containing 579 target genes, 15 housekeeping genes, 8 negative controls and 6 positive controls, as described previously.⁵

Statistical analysis

All plots were generated with GraphPad Prism v5.0. TCR sequencing analysis was performed using the Analyzer website (Adaptive Biotechnologies, Seattle, WA). For gene expression analysis, the raw. RCC files from nCounter system were QCed using NanoStringNorm version 1.1.21, under R version 3.2.0 (2015-04-16). The normalization of the expression was performed based on both the geometric means of the housekeeping genes, and the sum of expression of each sample. The statistical analysis was performed on the log₂-transformed expression with 2 sample t-test and unequal variance. The resulting p-values were adjusted through Benjamini-Hochberg procedure to account for multiple testing.

Results

Clinical presentation

The patient was an 80 year-old man with past oncologic history of resected Gleason 7 prostatic adenocarcinoma in 1995 and low grade B cell lymphoma treated curatively in 2012 with rituximab. Cardiovascular past medical history included coronary

artery disease with a bypass grafting in 1998 and chronic atrial fibrillation. The patient was diagnosed with primary cutaneous melanomas of the right low back in 2000 and the left shoulder in 2010. In 2013, surveillance imaging demonstrated a new left-sided 3.3 cm perihilar mass, a 3 cm left upper lobe lung nodule, and several enlarged mediastinal lymph nodes. Biopsy of the lung nodule confirmed metastatic melanoma. Clinical molecular testing was negative for *BRAF*, *NRAS* or *KIT* mutations. No other metastases were detected on imaging of the full body. The patient started treatment with ipilimumab 3 mg/kg given every 3 weeks. Sixteen days after the second ipilimumab treatment, the patient presented to an outside hospital with progressive shortness of breath and fatigue. Initial evaluation showed elevated B-type natriuretic peptide (BNP) of 2,222 pg/ml (normal range 15–121), consistent with congestive heart failure. No cardiac enzymes were sent, but a 2-D transthoracic echocardiogram showed an ejection fraction of 40–45% with stage III diastolic dysfunction and restrictive pattern. The patient was also noted to have elevated liver function tests, including aspartate aminotransferase (AST) of 679 IU/L (normal range 10–58), alanine aminotransferase (ALT) of 775 IU/L (normal range 5–50), and total bilirubin (BILI) of 2.5 mg/dL (normal range 0.2–1.2) (Fig. 1A, Supplemental Fig. 1). As serum serologies were negative for Hepatitis A, B, or C infection, the findings were felt to be consistent with autoimmune hepatitis. The patient was treated initially with intravenous (IV) corticosteroids and then converted to oral prednisone. The patient was discharged on hospital day 4. On the day of discharge, the BNP remained elevated, but the AST (138 IU/L), ALT (643 IU/L), and BILI (1.8 mg/DL) were markedly improved (Fig. 1A, Supplemental Fig. 1).

Two days later the patient presented to our center as scheduled for evaluation and ipilimumab treatment. As the patient remained dyspneic, treatment was held and the patient was admitted for further evaluation and management. Initial testing of cardiac enzymes revealed elevated Troponin-I (TNI) of 2.18ng/ml (normal range 0–0.03), creatine kinase myocardial b (CK-MB) of 15.9ng/ml (normal range 0.6–6.3), and normal total creatine kinase (CK) of 82U/L (normal range 55–170) (Fig. 1A, Supplemental Fig. 1). A CT scan of the chest demonstrated reduced size of the perihilar mass and left upper lobe lung mass, resolution of mediastinal lymphadenopathy, a small new left pleural effusion, and no evidence of pneumonitis or pneumonia (Fig. 1B). Over the next 7 days, the patient's liver enzymes progressively improved to near-normal levels with continued prednisone treatment. However, cardiac enzymes remained significantly elevated (Fig. 1A, Supplemental Fig. 1). A myocardial perfusion study revealed a fixed perfusion defect in the anterior wall on both stress and resting images, compatible with prior myocardial infarction, with no evidence of acute ischemia. On day 26 of cycle 2 of ipilimumab, cardiac enzymes remained elevated with a TNI of 3.7 ng/ml and CK-MB of 26.6ng/ml (Fig. 1A, Supplemental Fig. 1). Though prior electrocardiograms (EKG) showed no sign of myocarditis, an EKG on day 28 of cycle 2 of ipilimumab showed features compatible with myocarditis, including new diffuse ST segment elevation (Supplemental Fig. 2). This is consistent with EKG changes being a late manifestation of myocarditis. The patient's prednisone was changed to IV dexamethasone. Unfortunately, later

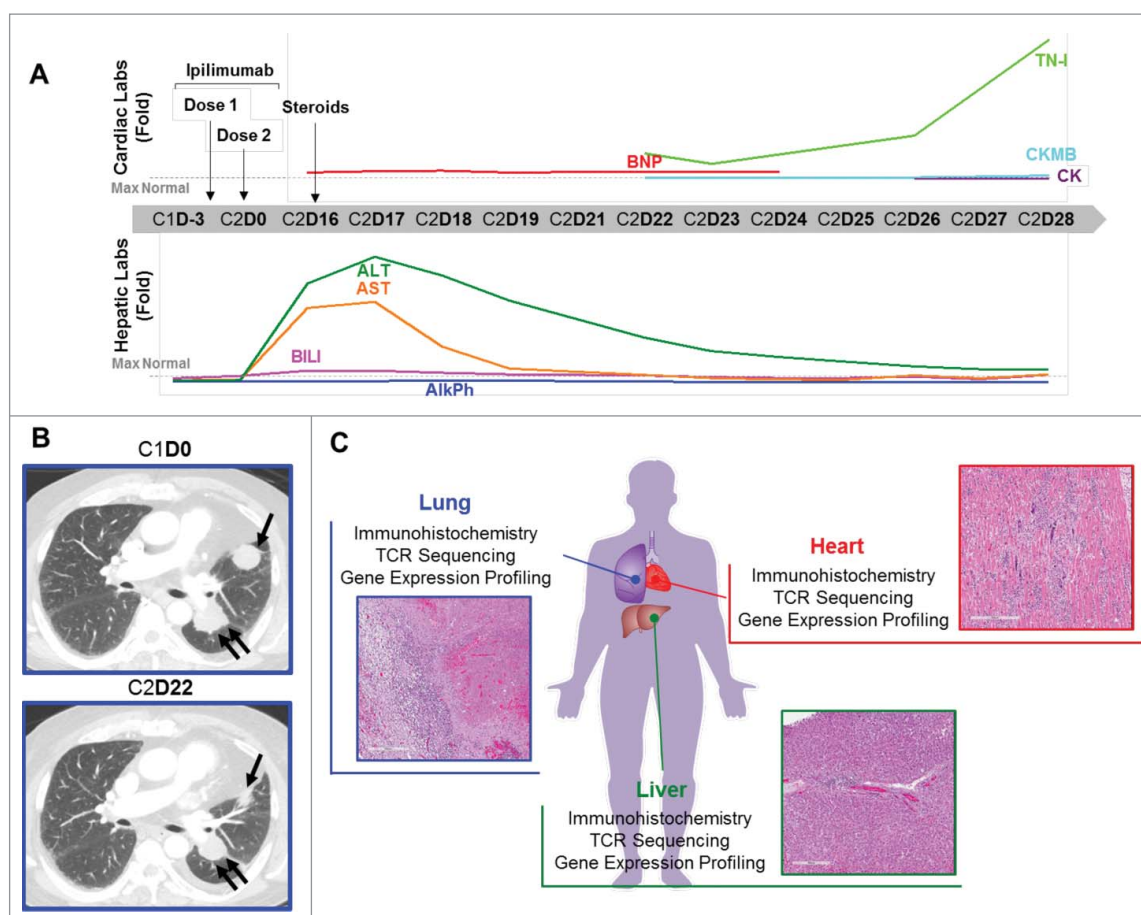


Figure 1. Autoimmune myocarditis in a patient with melanoma treated with ipilimumab. (A) Cardiac and hepatic function testing results over the course of therapy with ipilimumab. Graphs show results as fold-change for BNP, TN-I, CKMB, CK, BILI, ALT, AST, and AlkPh; horizontal dashed line indicates the upper limit of normal for each test. X-axis, day of ipilimumab treatment cycle (Cycle 1 = C1, Cycle 2 = C2). Arrows indicate the timing of ipilimumab doses and the start of corticosteroids. (B) Computerized tomography images of the lung metastasis before ipilimumab and after 2nd treatment. (C) Experimental plan and histological images of the heart, lung, and liver which were studied by immunohistochemistry, TCR sequencing, and gene expression profiling.

that day the patient developed sustained ventricular tachycardia, which degenerated to ventricular fibrillation followed by asystole. The patient's family agreed to post-mortem examination of the heart, liver, and lungs (Fig. 1C). Additional clinical details of the patient's case were previously reported.⁷

Clinical and pathological assessment

Autopsy examination of the heart identified cardiomegaly (890 g) with left ventricular hypertrophy (2.0 cm), with diffuse mottling of the myocardium and fusion of the pericardium to the epicardium, with significant fibrosis. The lung showed 2 nodules in the left side and one in the right side (Fig. 1B). Hepatomegaly was present. Microscopic evaluation revealed the left lung nodules to be entirely necrotic tumor surrounded by a moderate lymphohistiocytic infiltrate at the interface between the nodule and the normal lung parenchyma; the right lung nodule showed dense fibrosis and extensive calcification with no tumor cells. In the liver there was a mild portal lymphocytic infiltration, vascular congestion and associated zone III necrosis. The myocardium demonstrated a diffuse moderate to intense interstitial infiltrate composed of lymphocytes, a great number of multinucleated giant cells, and occasional eosinophils (Fig. 1C). The giant cells were positive for CD68 by IHC, confirming their histiocytic origin. Heart tissue was

cultured and showed no evidence of aerobic and anaerobic bacteria, acid-Fast Bacilli, or fungi. Aerobic blood cultures were negative, as were viral cultures for adenovirus, cytomegalovirus, herpes simplex virus, and varicella zoster. Together, the findings supported a diagnosis of autoimmune giant cell myocarditis.

Immune profiling reveals a predominant CD4⁺ T cell infiltrate in the myocardial tissue

Immunohistochemical (IHC) staining was performed for immune cell surface markers on 10 representative regions of heart tissue, liver tissue, and one of the necrotic melanoma lung metastases to determine the relative composition of the immune infiltrates at each site (Fig. 2A–F). A predominant CD3⁺ T cell infiltrate was present in the heart and lung (Fig. 2A). The vast majority of the T cell infiltrate in the heart consisted of CD4⁺ T cells. There were very few CD8⁺ T cells detected in the heart or liver, but they were the predominant immune cell population in the area of the lung containing the necrotic metastases (Fig. 2B–C). Few CD20⁺ B cells were detected, with the highest number found in the lung. FoxP3 and CD45RO staining were performed to identify regulatory T cells (Treg) and antigen-experienced T cells, respectively. This analysis showed almost no FoxP3 expression in heart and liver

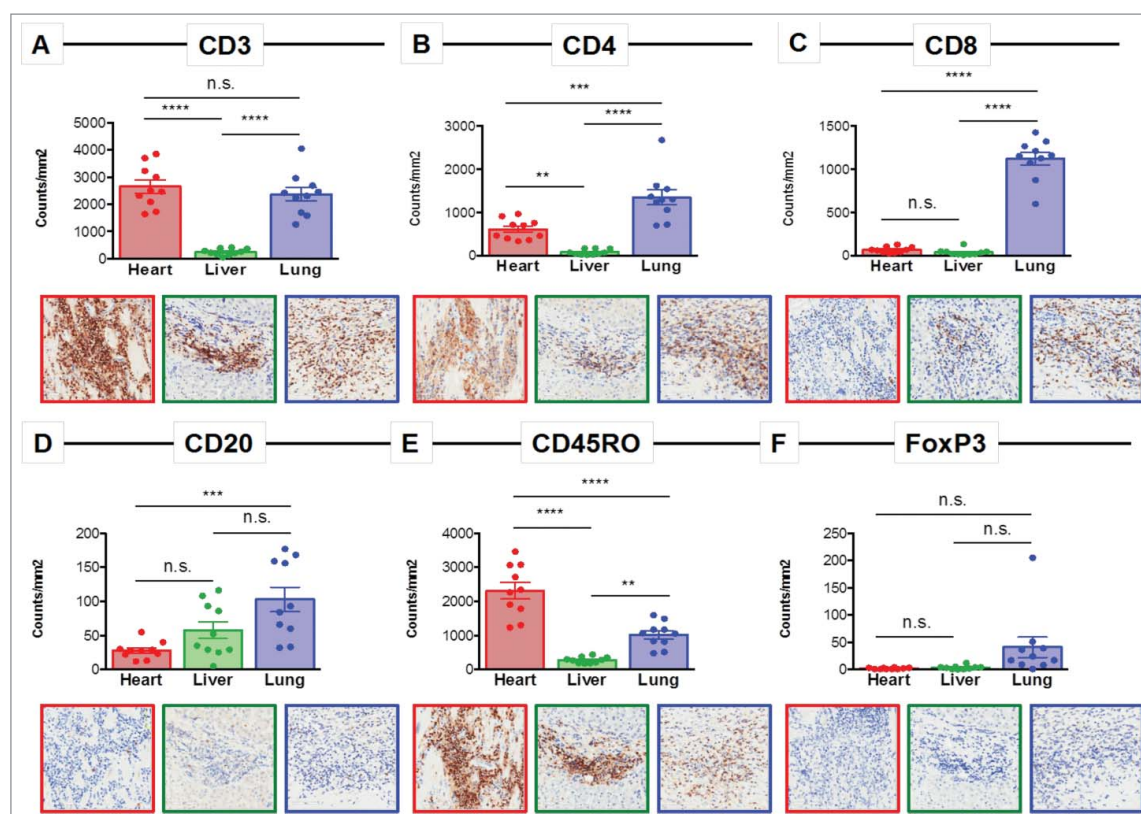


Figure 2. Immune profiling of the inflamed heart reveals a CD4-dominated T cell infiltrate. Representative immunohistochemistry images and quantification of 10 regions for (A) CD3, (B) CD4, (C) CD8, (D) CD20, (E) CD45RO, and (F) FoxP3 in the heart, liver, and lung. n.s. = not significant; ** = $p < 0.01$; *** = $p < 0.001$; **** = $p < 0.0001$.

tissue and low expression in the lung metastasis and CD45RO expression was highest in the heart (Fig. 2D–F).

T cell receptor sequencing confirms presence of a low clonality T cell infiltrate in the inflamed heart

Sequencing of the CDR3 variable region of the β chain of the T cell receptor was performed to characterize the T cell repertoire of the lymphocytic infiltration in the heart, and for comparison to those detected in the liver (resolving autoimmune inflammation) and the responding lung metastases. This analysis demonstrated that the clonality of the T cell infiltrate was highest in the responding lung metastasis, but very low in the heart and liver tissues (Fig. 3A). Comparative analysis of the heart, liver and lung demonstrated that only 1% of T cell clones were detectable in all organs, with the highest proportion of unique T cell clones observed in the lung (69.5%) (Fig. 3B). Very few T cell clones were detected in the liver ($n = 194$) compared with the heart ($n = 3,147$) and the lung ($n = 8,416$), and the clones detected in the liver showed very little overlap with those in the heart (1.2%) or in the lung metastasis (1.3%) (Fig. 3B). More overlap ($n = 1,044$; 9.9%) of T cell repertoire was observed between the heart tissue and the lung metastasis.

To better understand the nature of the overlap between the sites, we next investigated the highest frequency T cell clones considered most likely to be expanding and involved in antigen-specific responses. To do so, the 100 most prevalent T cell clones detected in the patient were ranked and their frequency was quantified in each tissue (Fig. 3C). The highest frequency

clones were found at the highest prevalence in the lung, consistent with the clonality and clinical response observed. All of the top 100 clones were also detectable in the heart but at low frequency, in line with the overall low clonality observed (Fig. 3C). The 2 highest frequency clones were not detected in the liver, further underscoring the differences in immune infiltrates between these organs. The results suggest a heterogeneous T cell repertoire across these organs, with a clonal infiltrate in the responding lung metastasis, and extremely diffuse and non-clonal infiltrate in the heart and liver. The patterns in the heart and liver are consistent with a lack of antigen-specific responses, and suggest that the myocardial immune infiltrate could have been triggered by non-specific infiltration of immune cells through chemotaxis.

Differential expression of immune-related genes reveals increased expression of CXCR3-axis chemokines in the heart

The expression of 579 immune-related genes was characterized in RNA from heart tissue, liver tissue, and a lung metastasis to evaluate factors in each microenvironment that may have influenced the observed differential immune responses and sensitivity to steroids. Comparison of gene expression in heart tissue versus non-heart tissue (liver and lung) identified *CXCL11*, *IL12RB1*, *TNFRSF4*, *IRF1*, *CD8B*, *CCL13*, *IL2RB*, *IDO1*, *CXCR3*, *EBI3*, *CCL19*, and *IRF4* as the genes most overexpressed in the heart compared with the liver and lung, while *C1S* and *CXCL13* were the genes most decreased in the heart

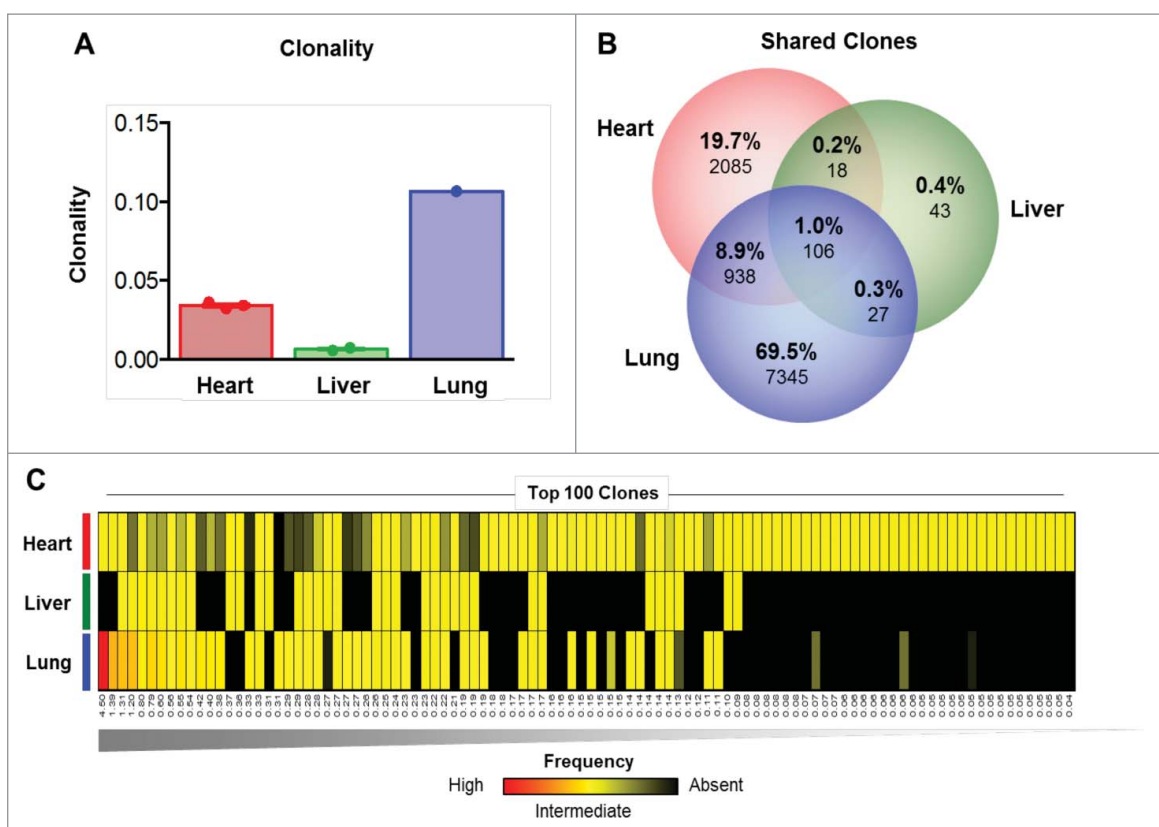


Figure 3. TCR sequencing suggests a polyclonal T cell infiltrate in the heart. (A) Clonality of the T cell repertoire in the heart, liver and lung tissues. (B) Overlap in the T cell repertoire between the heart, liver and lung. (C) Top 100 clones detected ranked by highest frequency ($n = 1$, left) to lowest frequency ($n = 100$, right) as detected in the heart, liver and lung. Red = high frequency, Yellow = low frequency, Black = absence.

(Fig. 4A–D, Supplemental Table S1). Comparison of the heart to the liver identified 55 significantly differentially-expressed genes, while comparison to the lung metastasis identified 16 differentially-expressed genes. Increased expression of the chemokines *CXCL9* ($p < 0.0001$) and *CXCL11* ($p < 0.0001$), and their receptor *CXCR3* ($p < 0.0001$), was also detected in the heart compared with both liver and lung (Fig. 4E–G).

Analysis of checkpoint molecules revealed that *PDCDI* (PD-1) ($p < 0.001$), *LAG3* ($p < 0.0001$) and *CD274* (PD-L1) ($p < 0.001$) were increased in the heart compared with both the liver and lung (Supplemental Fig. S3A–C). Higher expression of the MHC class II molecules *HLA-DRB1* ($p < 0.0001$) and *HLA-DRB3* ($p < 0.0001$) was also observed in the heart tissue (Supplemental Fig. S3D–E).

Discussion

Autoimmune myocarditis is a rare but life-threatening complication of immunotherapy. An improved understanding of the pathogenesis of autoimmune myocarditis may lead to better treatments. Our comparative analysis of post-mortem tissue from responding melanoma lung metastases, controlled liver inflammation, and uncontrolled myocarditis from a patient treated with ipilimumab demonstrates the heterogeneity of the immune response in different organ sites that can occur with checkpoint inhibitor immunotherapy.

While there have been other reports characterizing autoimmune myocarditis following checkpoint inhibitor therapy,^{4,8–12} to our knowledge this is the first study to characterize the

immune features of myocarditis with single-agent ipilimumab treatment, and the first to identify evidence of giant cell myocarditis. Giant cell myocarditis (GCM) is a form of autoimmune myocarditis with worse prognosis than lymphocytic myocarditis, with suboptimal responsiveness to conventional immunosuppressive treatments. Compared to lymphocytic myocarditis, GCM myocarditis is rapidly progressive with a high rate of mechanical circulatory support and/or cardiac transplantation, and a 5-year transplant-free survival rate of 52%.¹³ Histologically, GCM is characterized by a lymphocytic infiltration with multinucleated giant cells and myocyte necrosis and poses significant clinical challenges due both to its very aggressive clinical course and because definitive diagnosis generally relies on endomyocardial biopsies or autopsy studies.¹⁴

Few cases of myocarditis have been reported following ipilimumab.^{4,9,10,15,16} One study reported a myocarditis case secondary to the combination of ipilimumab and nivolumab treatment in a metastatic melanoma patient with clinical symptoms that included chest pain, fever, and malaise, which resolved with corticosteroids and suspension of the immunotherapy. No further histopathological or molecular characterization of the myocarditis was reported.¹⁶ Another report described autoimmune myocarditis in a patient undergoing pembrolizumab treatment of metastatic uveal melanoma who had previously received 4 cycles of ipilimumab. A cardiac biopsy revealed a lymphocytic myocarditis predominantly composed of CD8+ T cells, and the patient improved with corticosteroid treatment and withdrawal of pembrolizumab.⁸ Another study reported a fatal case of a melanoma patient

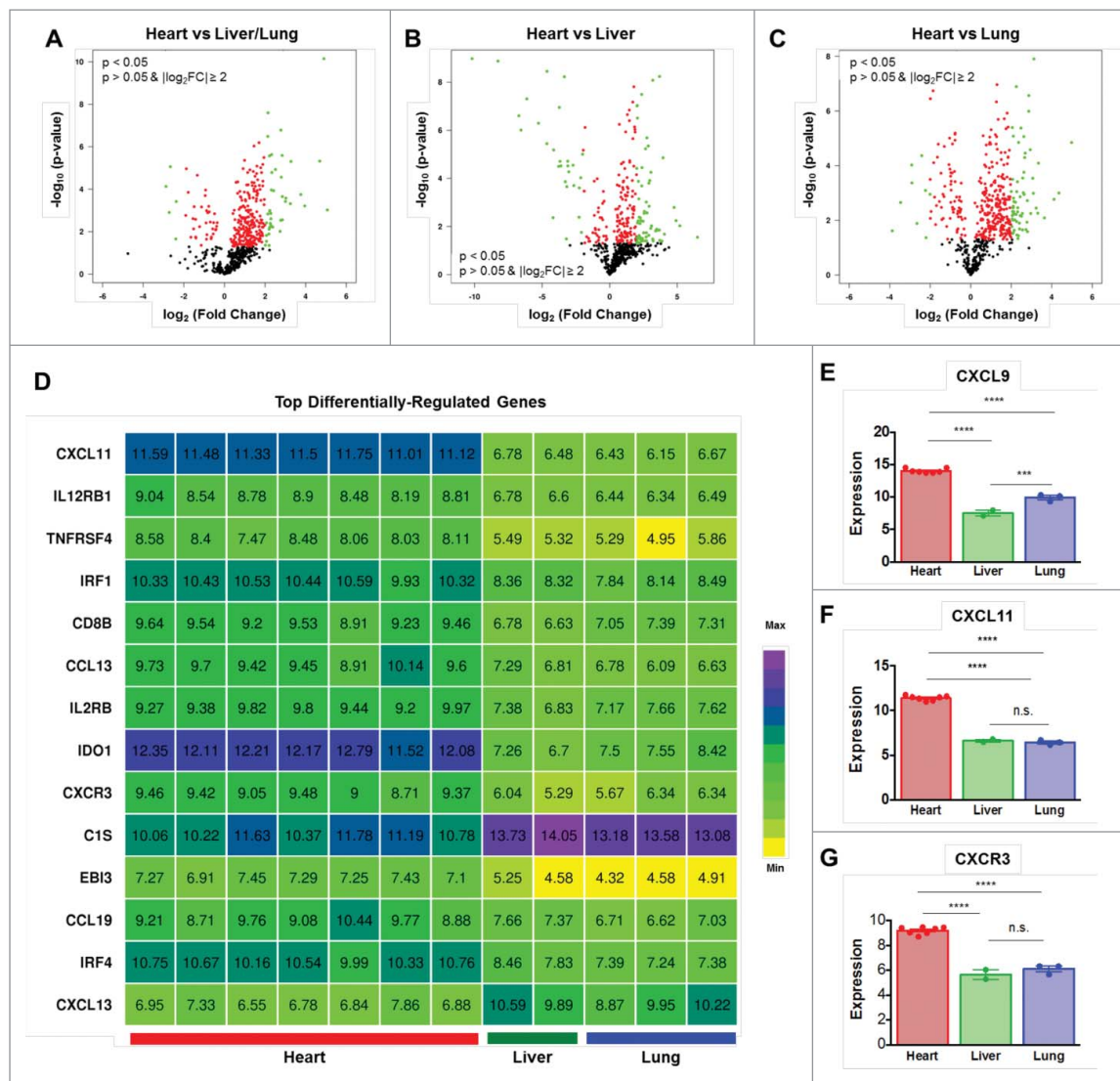


Figure 4. Gene expression profiling demonstrates increased CXCR3-axis chemokine expression in the heart. Gene expression profiling showing differentially expressed genes in comparing (A) multiple samples of heart tissue to non-heart (lung/liver) tissue samples, (B) the heart to the liver, and (C) the heart to the lung. (D) Most differentially expressed genes detected when comparing the heart, liver, and lung. Normalized expression levels of (E) CXCL9, (F) CXCL11, and (G) CXCR3. n.s. = not significant; *** = $p < 0.001$; **** = $p < 0.0001$.

treated with anti-CTLA-4 followed by anti-PD-1 who developed aseptic meningioencephalitis and myocarditis, with both sites showing an infiltration comprised predominantly of CD8 T cells.¹⁵

Recently, deeper immune analysis of 2 melanoma patients who developed fatal myocarditis after treatment with the combination of ipilimumab and nivolumab has been reported.⁹ Characterization of post-mortem tissues found that the cells infiltrating the heart were either CD3+ T cells or CD68+ myeloid cells. Further profiling revealed that the T cell infiltrate consisted of both CD4+ and CD8+ T cells. In contrast, in our patient treated with single-agent ipilimumab we observed that the cardiac infiltrate consisted predominantly of CD4+ T cells, with very few CD8+ T cells. Notably, our findings in this patient treated with single-agent ipilimumab corroborate work in animal models that supported a more important role for CD4+ than CD8+ T cells in autoimmune toxicity related to loss of CTLA-4.^{17,18} Although definite conclusions require analysis of additional patients, the results support that

the pathogenesis of autoimmune myocarditis may differ between patients receiving anti-PD-1 and anti-CTLA-4 immunotherapy.

TCR profiling was also performed in the 2 patients with fatal myocarditis following combination ipilimumab and nivolumab treatment.⁹ Although clonality was not reported, in one patient the most prevalent T cell clone in the heart was also among the most prevalent in the tumor, and had expanded upon treatment. However, the most prevalent T cell clone in the heart of the other patient was not detected in pre-treatment tumor tissue. In our patient we observed striking differences in the T cell repertoires of the heart (active myocarditis), liver (resolved hepatitis) and lung metastases (clinically responding). A high clonality was observed in the responding lung, as would be expected. However, low clonality was detected in the heart and liver. Interestingly, the heart tissue and lung metastasis had some overlap of T cell repertoires, suggesting that T cells infiltrating and responding to the lung metastases may also have contributed to the autoimmune myocarditis. This possibility is

supported by the ubiquitous CD45RO expression detected on T cells in the heart, which suggests that these cells were antigen-experienced rather than naïve. The secondary inflammation of the heart is also supported by the elevated expression of PD-1, PD-L1, and LAG-3 detected in the heart tissue, as these markers may be induced in the context of a normal negative feedback loop to prevent or minimize autoimmune responses in an inflamed environment, as occurs with prolonged exposure to IFN- γ . The high expression of IDO1 in the heart tissue is also in line with deployment of an inflammation-induced negative feedback loop. Similar immunosuppressive proteins were also observed in the cardiac tissue of the patients that had received combination ipilimumab and nivolumab.⁹ Finally, we also detected upregulation of TNFRSF4, also termed OX40, in the heart tissue. Contrary to PD-1 and CTLA-4, OX40 is a T cell agonist that can induce T cell responses upon ligation, and thus it could have contributed to the increased inflammation seen in the heart.¹⁹

We also detected increased expression of chemokines that could have promoted T cell trafficking into the heart. CXCL9 and CXCL11 were among differentially-expressed genes in the heart compared with the liver and lung, and CXCR3, their receptor, was also overexpressed in the heart. CXCR3 is induced on T cells upon activation.²⁰ As the T cells in the heart demonstrated ubiquitous expression of CD45RO, it is possible that the cells were activated in the response to the patient's lung metastases, which induced CXCR3 expression. This effect could have favored subsequent trafficking to the CXCL9/CXCL11-rich myocardium. Of note, other cytokines such as IFN- γ could also have played a role in this context, but these findings must be further validated to confirm these associations.

In summary, our studies present new insights into the pathogenesis of autoimmune myocarditis with single agent ipilimumab, which is approved by the FDA for both stage III and stage IV melanoma. The novel finding of giant-cell myocarditis is consistent with the failure of steroids to resolve this toxicity in this patient, and combined treatment with corticosteroids, azathioprine, and cyclosporine should be considered in future patients that are steroid-refractory.¹⁷ Notably, we found that the immune infiltrate in the heart was comprised largely of CD4+ T cells, which contrasts with the infiltrate observed in this patient's steroid-responsive liver tissue and shrinking lung metastases. This finding also differs from previously reported CD8+ T cell-predominant myocarditis in patients treated with anti-PD-1 containing regimens. Finally, our results suggest that the CXCR3-axis could be a target to reverse ipilimumab-induced autoimmune myocarditis. Together our analyses demonstrate that heterogeneous immune responses can occur in normal tissues with checkpoint inhibitor therapy, as has been observed in synchronous metastatic tumors.²¹

Disclosures



ZAC is an employee of MedImmune and owns stock or options in AstraZeneca. HT is a consultant for Bristol-Myers Squibb and Novartis. AJL is a consultant for MedImmune, Bristol-Myers Squibb, Novartis, and Merck and has received research support from AstraZeneca/MedImmune. JAW has honoraria from speakers' bureau of Dava Oncology, Bristol-Myers

Squibb and Illumina and is an advisory board member for GlaxoSmithKline, Novartis, and Roche/Genentech. MAD is an advisory board member for Bristol-Myers Squibb, GlaxoSmithKline, Roche/Genentech, Novartis and Sanofi-Aventis and has received research support from GlaxoSmithKline, Roche/Genentech, Sanofi-Aventis, Oncocyte, Myriad, and AstraZeneca. The remaining authors declare no financial conflicts of interest.

Financial support

This work was supported by the Dr. Miriam and Sheldon G. Adelson Medical Research Foundation and philanthropic contributions to The University of Texas MD Anderson Cancer Center Melanoma Moon Shot Program.

ORCID

Alexandre Reuben  <http://orcid.org/0000-0003-4510-0382>
Alexander J. Lazar  <http://orcid.org/0000-0002-6395-4499>

References

- Hodi FS, O'Day SJ, McDermott DF, Weber RW, Sosman JA, Haanen JB, Gonzalez R, Robert C, Schadendorf D, Hassel JC, et al. Improved survival with ipilimumab in patients with metastatic melanoma. *N Engl J Med*. 2010;363:711-23. doi:10.1056/NEJMoa1003466. PMID:20525992
- Schadendorf D, Hodi FS, Robert C, Weber JS, Margolin K, Hamid O, Patt D, Chen TT, Berman DM, Wolchok JD. Pooled Analysis of long-term survival data from phase II and Phase III trials of ipilimumab in unresectable or metastatic melanoma. *J Clin Oncol*. 2015;33:1889-94. doi:10.1200/JCO.2014.56.2736. PMID:25667295
- Robert C, Thomas L, Bondarenko I, O'Day S, Weber J, Garbe C, Lebbe C, Baurain JF, Testori A, Grob JJ, et al. Ipilimumab plus dacarbazine for previously untreated metastatic melanoma. *N Engl J Med*. 2011;364:2517-26. doi:10.1056/NEJMoa1104621. PMID:21639810
- Eggermont AM, Chiarion-Sileni V, Grob JJ, Dummer R, Wolchok JD, Schmidt H, Hamid O, Robert C, Ascierto PA, Richards JM, et al. Adjuvant ipilimumab versus placebo after complete resection of high-risk stage III melanoma (EORTC 18071): A randomised, double-blind, phase 3 trial. *Lancet Oncol*. 2015;16:522-30. doi:10.1016/S1470-2045(15)70122-1. PMID:25840693
- Chen PL, Roh W, Reuben A, Cooper ZA, Spencer CN, Prieto PA, Miller JP, Bassett RL, Gopalakrishnan V, Wani K, et al. Analysis of immune signatures in longitudinal tumor samples yields insight into biomarkers of response and mechanisms of resistance to immune checkpoint blockade. *Cancer Discov*. 2016;6:827-37. doi:10.1158/2159-8290.CD-15-1545. PMID:27301722
- Cooper ZA, Frederick DT, Juneja VR, Sullivan RJ, Lawrence DP, Piris A, Sharpe AH, Fisher DE, Flaherty KT, Wargo JA. BRAF inhibition is associated with increased clonality in tumor-infiltrating lymphocytes. *Oncoimmunology*. 2013;2:e26615. doi:10.4161/onci.26615. PMID:24251082
- Heinzerling L, Ott PA, Hodi FS, Husain AN, Tajmir-Riahi A, Tawbi H, Pauschinger M, Gajewski TF, Lipson EJ, Luke JJ. Cardiotoxicity associated with CTLA4 and PD1 blocking immunotherapy. *J Immunother Cancer*. 2016;4:50. doi:10.1186/s40425-016-0152-y. PMID:27532025
- Laubli H, Balmelli C, Bossard M, Pfister O, Glatz K, Zippelius A. Acute heart failure due to autoimmune myocarditis under pembrolizumab treatment for metastatic melanoma. *J Immunother Cancer*. 2015;3:11. doi:10.1186/s40425-015-0057-1. PMID:25901283
- Johnson DB, Balko JM, Compton ML, Chalkias S, Gorham J, Xu Y, Hicks M, Puzanov I, Alexander MR, Bloomer TL, et al. Fulminant myocarditis with combination immune checkpoint blockade. *N Engl J Med*. 2016;375:1749-55. doi:10.1056/NEJMoa1609214. PMID:27806233
- Geisler BP, Raad RA, Esaian D, Sharon E, Schwartz DR. Apical ballooning and cardiomyopathy in a melanoma patient treated with

- ipilimumab: A case of takotsubo-like syndrome. *J Immunother Cancer*. 2015;3:4. doi:10.1186/s40425-015-0048-2. PMID:25705383
11. Cheng F, Loscalzo J. Autoimmune cardiotoxicity of cancer immunotherapy. *Trends Immunol*. 2017;38:77-8. doi:10.1016/j.it.2016.11.007. PMID:27919707
 12. Heinzerling L, Goldinger SM. A review of serious adverse effects under treatment with checkpoint inhibitors. *Curr Opin Oncol*. 2017;29:136-44. doi:10.1097/CCO.000000000000358. PMID:28059853
 13. Kandolin R, Lehtonen J, Salmenkivi K, Raisanen-Sokolowski A, Lommi J, Kupari M. Diagnosis, treatment, and outcome of giant-cell myocarditis in the era of combined immunosuppression. *Circ Heart Fail*. 2013;6:15-22. doi:10.1161/CIRCHEARTFAILURE.112.969261. PMID:23149495
 14. Xu J, Brooks EG. Giant cell myocarditis: A brief review. *Arch Pathol Lab Med*. 2016;140:1429-34. doi:10.5858/arpa.2016-0068-RS. PMID:27922771
 15. Koelzer VH, Rothschild SI, Zihler D, Wicki A, Willi B, Willi N, Voegeli M, Cathomas G, Zippelius A, Mertz KD. Systemic inflammation in a melanoma patient treated with immune checkpoint inhibitors-an autopsy study. *J Immunother Cancer*. 2016;4:13. doi:10.1186/s40425-016-0117-1. PMID:26981243
 16. Mehta A, Gupta A, Hannallah F, Koshy T, Reimold S. Myocarditis as an immune-related adverse event with ipilimumab/nivolumab combination therapy for metastatic melanoma. *Melanoma Res*. 2016;26:319-20. doi:10.1097/CMR.0000000000000251. PMID:27110676
 17. Cooper LT Jr, Berry GJ, Shabetai R. Idiopathic giant-cell myocarditis—natural history and treatment. Multicenter giant cell myocarditis study group investigators. *N Engl J Med*. 1997;336:1860-6. doi:10.1056/NEJM199706263362603. PMID:9197214
 18. Yuan Z, Shioji K, Kishimoto C. Immunohistological analyses of myocardial infiltrating cells in various animal models of myocarditis. *Exp Clin Cardiol*. 2003;8:13-6. PMID:19644581
 19. Fousteri G, Dave A, Morin B, Omid S, Croft M, von Herrath MG. Nasal cardiac myosin peptide treatment and OX40 blockade protect mice from acute and chronic virally-induced myocarditis. *J Autoimmun*. 2011;36:210-20. doi:10.1016/j.jaut.2011.01.006. PMID:21333491
 20. Hirota Y, Osuga Y, Koga K, Yoshino O, Hirata T, Morimoto C, Harada M, Takemura Y, Nose E, Yano T, et al. The expression and possible roles of chemokine CXCL11 and its receptor CXCR3 in the human endometrium. *J Immunol*. 2006;177:8813-21. doi:10.4049/jimmunol.177.12.8813. PMID:17142784
 21. Reuben A, Spencer CN, Prieto PA, Gopalakrishnan V, Reddy SM, Miller JP, Mao X, De Macedo MP, Chen J, Song X, et al. Genomic and immune heterogeneity are associated with differential responses to therapy in melanoma. *npj Genomic Med*. 2017;2:10. doi:10.1038/s41525-017-0013-8